Journal of Applied Electrochemistry **30**: 1103–1108, 2000.

Kinetics and mechanism of the formation of doped skeletal copper catalysts: the effect of zincate compared to undoped and chromate-doped systems

A.J. SMITH, T. TRAN* and M.S. WAINWRIGHT
*School of Chemical Engineering and Industrial Chemistry, University of New South Wales, Sydney, Australia, 2052 (*author for correspondence)*

Received 18 January 2000; accepted in revised form 9 May 2000

Key words: de-alloying, Raney®†, selective dissolution, structure, zinc additive

Abstract

Addition of zincate to the leach liquor for the preparation of skeletal copper increases the copper surface area; however it does not stabilize the structure against rearrangement. The leaching kinetics have been studied using a rotating disc electrode (RDE) at 269–293 K in 2–8 M NaOH and 0.0005–0.1 M Na_2ZnO_2. Zincate ions precipitate as zinc oxide, due to the local consumption of hydroxide ions near the leach front as the aluminium dissolves. This oxide hinders the aluminium dissolution, slowing the leaching rate. It also hinders copper dissolution/redeposition and prevents copper diffusion, thus reducing the structural rearrangement significantly, and causing the formation of a much finer copper structure with increased surface area. The zinc oxide redissolves as the leach front passes, releasing the copper to rearrange once more, thereby allowing the surface area to decrease with time. The activation energy for leaching was found to be 84 ± 6 kJ mol^{-1}.

List of symbols

A_{disc}	flat geometric surface area of the rotating alloy disc (m^2)
$\alpha_{H_2,Cu}$	transfer coefficient for H_2 evolution on Cu
E	actual potential (V)
$E^{0'}_{H_2}$	formal potential for the hydrogen evolution reaction (V)
F	faradaic constant (96 486 C mol^{-1})
$k^0_{H_2,Cu}$	standard rate constant for hydrogen evolution on pure copper
K	proportionality constant
k_d, k_r	rate constants for the leaching and rearrangement reactions, respectively
n_a	number of electrons transferred in the rate limiting step
R	gas constant (8.314 J mol^{-1} K^{-1})
$r_{L,0}$	initial ligament radius (m)
T	absolute temperature (K)
t	time (min)
x	rearrangement exponential

1. Introduction

The selective dissolution of aluminium from a copper–aluminium alloy leaves a highly porous copper residue that is an active hydrogenation catalyst known as skeletal or Raney® copper [1–3]. The addition of dopants can increase the activity and selectivity of these catalysts towards particular reactions, for example methanol synthesis from syn-gas [4–6]. The most popular dopant for the methanol synthesis reaction has been zinc, either added to the precursor alloy before leaching, or preferably to the leachant solution as zincate [7, 8]. The increased activity of doped skeletal catalysts has been attributed to an increased surface area [9].

A previous paper [10], based on electrochemistry, established the mechanism of the formation of the skeletal copper structure upon removal of two-thirds of the atoms from the $CuAl_2$ alloy. The mechanism involved the dissolution of both components, followed by the redeposition of the copper. The dissolution/redeposition of the copper was also the main cause of structural rearrangement which reduced the surface area with time. Surface and/or volume diffusion of copper was found to play a minor role.

Another paper [11], in extension to this previous work, established that the chromate-doped system could be studied in the same way. Chromate ions reduced to chromium(III) oxide during the leaching of aluminium, depositing on the leached copper and unleached alloy surfaces. This slowed the leaching rate, but more importantly it hindered the dissolution/redeposition mechanism of the copper structure formation/rearrangement. A finer copper structure resulted, having a higher surface area and activity.

† Raney® is a registered trademark of W.R. Grace & Co

Zincate addition has also been found to increase the surface area of the catalyst; however the structure still suffers from reduction in surface area over time [9]. The current work is a further extension to the two previous papers, using the established reasoning to understand the more complicated zincate system. The kinetics of leaching and the effect of zincate on the mechanism are studied and compared to both the undoped and chromate-doped systems.

2. Experimental details

The experimental procedures for this work have been described previously [11], with zincate being used in place of chromate. The precursor alloy for all experiments was supplied by Riverside Metal Industrial Pty Ltd and consisted of 52.17% w/w Cu, remainder Al. The leaching solution was 6 M NaOH + 0.06 M Na_2ZnO_2 at 274 K unless otherwise specified. The temperature was varied from 269 K to 293 K, the sodium hydroxide concentration from 2 M to 8 M, and the sodium zincate concentration from zero to 0.1 M.

All measurements in this work are within a maximum of 10% error, and all potentials are reported against a Ag/AgCl reference electrode.

3. Results and discussion

3.1. *Structure*

To use the Focussed Ion Beam (FIB) miller to study the zincate-doped structure, the alloy was leached for three days rather than overnight. This was necessary to have a reasonable amount leached, as the leaching rate is much slower than either the undoped or chromate-doped systems (see Section 3.2). Even then, it was still difficult to obtain a profile image by viewing the side of a milled hole after a 'polishing mill'. For this reason, Figure 1(a) is an image taken from directly above the leached alloy surface, just after a light polishing mill has removed the top crust to reveal the internal structure.

The structure of zincate-doped skeletal copper (Figure 1(a)) was found to be much finer than the undoped catalyst (Figure 1(b)), yet retaining the same basic shape: a uniform three-dimensional network of fine ligaments. The scale was similar to the chromate-doped system (Figure 1(c)). It should be noted that with three days of leaching it is probable that the zincate-doped structure would have been much finer at the same time of leaching as the chromate-doped structure, since the former suffers from surface area loss with continued leaching whereas the latter does not [9]. The important points are that the structure is finer than the undoped catalyst (the cause of the increased surface area and hence activity of the catalyst) and it still retains the same basic shape which is important for applying the previously derived [10] Equation 1 for understanding the mechanism.

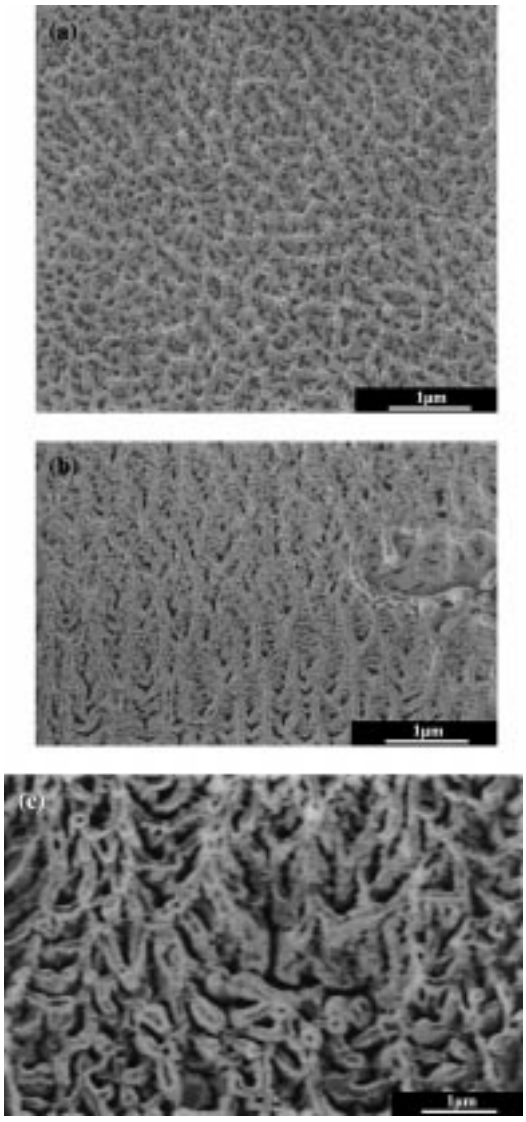

Fig. 1. Leached structures viewed by FIB at identical magnification. (a) zincate-doped structure, (b) chromate-doped structure [11] and (c) undoped structure [10].

3.2. *Leaching kinetics*

Similarly to the undoped and chromate-doped systems [10, 11], the aluminium leaching rate was constant (Figure 2) under the conditions used (0.005–0.1 M Na_2ZnO_2, 2–8 M NaOH, 269–293 K). The zincate concentration had a strong effect on the rate (Figure 3), slowing it with increased zincate concentration. The effect was much stronger than in the chromate system [11] and reached a maximum at higher zincate concentrations (above 0.04 M Na_2ZnO_2).

Figure 4 shows that the sodium hydroxide concentration did not significantly affect the leaching rate, which was also the case for the undoped and chromate-doped systems studied previously [10, 11]. However temperature did have an effect and an activation energy of 85 ± 6 kJ mol^{-1} was calculated from the Arrhenius plot in Figure 5. This compares with 74 ± 7 kJ mol^{-1} for the chromate system [11] and 69 ± 7 kJ mol^{-1} without additives [10].

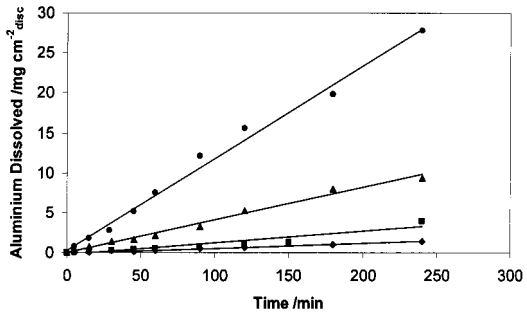

Fig. 2. Rate of leaching at various temperatures in 6 M NaOH + 0.025 M Na_2ZnO_2. Key: (◆) 269 K, (■) 274 K, (▲) 283 K and (●) 293 K.

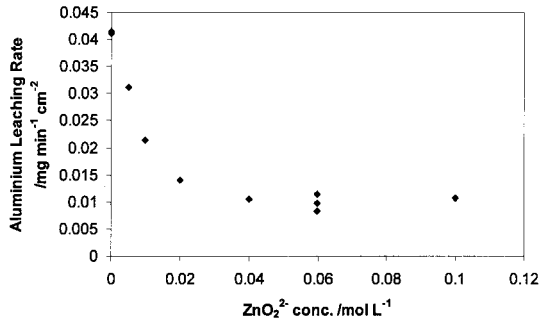

Fig. 3. Effect of zincate concentration on leaching rate (6 M NaOH, 274 K).

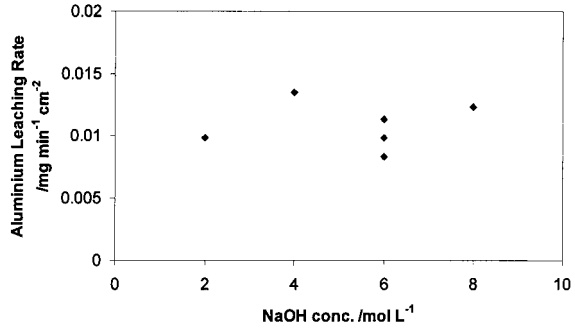

Fig. 4. Leaching rate is independent of hydroxide concentration in the presence of zincate.

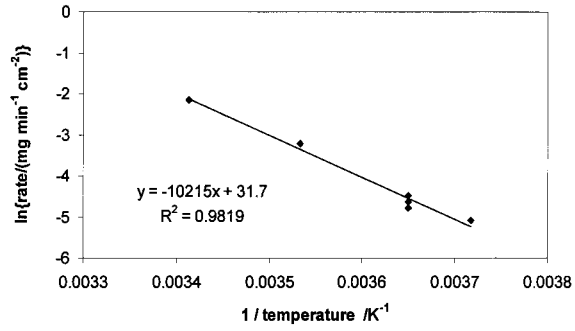

Fig. 5. Arrhenius plot for leaching in the presence of zincate.

3.3. *Applying the mechanism theory*

Equation 1, derived for the Raney® copper system without additives [10], relates the mixed corrosion potential of the dissolving alloy to time:

$$E = \frac{RT(1-x)}{\alpha_{H_2,Cu} n_a F} \ln(t) - \frac{RT}{\alpha_{H_2,Cu} n_a F} \times \ln\left(\frac{3A_{disc}\frac{dAl^{3+}}{dt} k_r (1-x)}{2k^0_{H_2,Cu} r_{L,0} K k_d}\right) + E^{0'}_{H_2} \quad (1)$$

The slope of a plot of E against $\ln(t)$ gives a value for x that corresponds to the mechanism of formation/rearrangement of the Raney® structure. Equation 1 was derived for a system with a constant leaching rate and equality between the hydrogen evolution current and the aluminium dissolution current. It was shown that the equation was applicable to the chromate system [11] as well, since it met these constraints. With the zincate system, the leaching rate is again constant (Figure 2) and the zincate ions cannot be reduced to zinc metal at the corrosion potentials measured [12, 13] (the current balance between aluminium and hydrogen holds). Therefore Equation 1 should apply equally well for this system. Figure 6 confirms this, although there is more scatter in the data than with the undoped and chromate-doped systems [10, 11]. The scatter arises from the mixed corrosion potential not rising steadily with time; possible causes of this will be discussed later.

For review, the value for x in Equation 1 indicates one of four types of rearrangement mechanisms: 1 = viscous flow; $\frac{1}{2}$ = dissolution/reprecipitation; $\frac{1}{3}$ = volume diffusion; $\frac{1}{4}$ = surface diffusion. There may be a combination of more than one of these main mechanisms, in which case x would take on an intermediate value. The value of x of ~0.5 for the undoped system [10] indicated primarily dissolution/reprecipitation of copper as the mechanism, which confirmed the proposals of Tomsett [14, 15] and Kalina et al. [18, 19].

The slope of E against $\ln(t)$ for the zinc system gives an x-value of about 0.3 (Figure 7). This compares to 0.5 for the undoped system [10] and 0.4 for the chromate

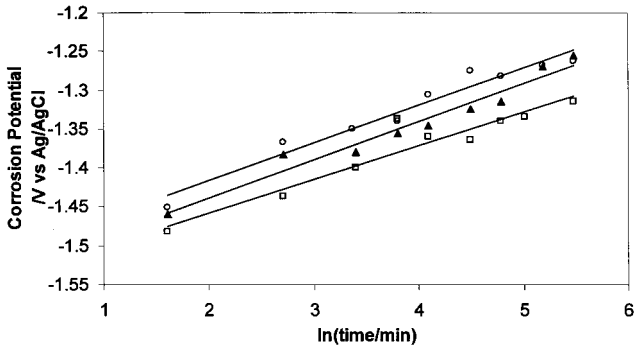

Fig. 6. Corrosion potential versus the logarithm of time is linear, verifying Equation 1. Key: (□) 274 K, (▲) 283 K and (○) 293 K.

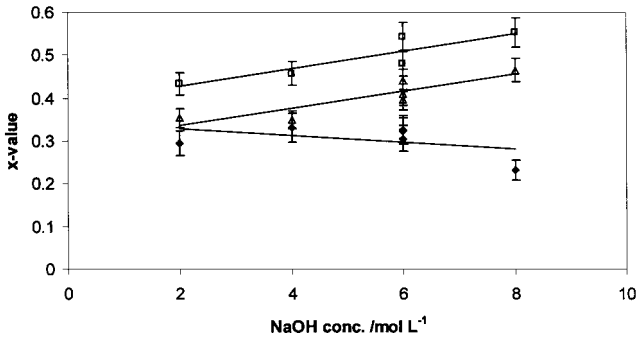

Fig. 7. The *x*-value is independent of hydroxide concentration in the presence of zincate. Non-zincate data from [10, 11]. Key: (◆) 0.06 M zincate, (△) 0.025 M chromate (□) no additives.

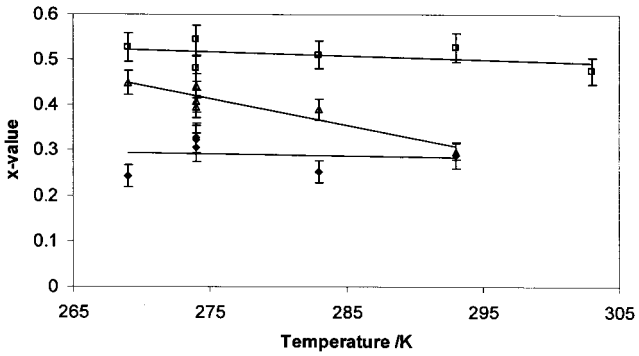

Fig. 8. The *x*-value is independent of temperature in the presence of zincate. Non-zincate data from [10, 11]. Key: (◆) 0.06 M zincate, (△) 0.025 M chromate (□) no additives.

system [11], indicating that there is a smaller proportion of dissolution/redeposition of copper in the formation/rearrangement mechanism in the presence of zincate.

In the presence of zincate the *x*-value showed a slight convex dependence on hydroxide concentration (Figure 7). In the undoped and chromate-doped systems, a linear dependence with hydroxide concentration indicated the presence of copper diffusion in the rearrangement mechanism. The amount of dissolution/redeposition of copper decreased as the hydroxide concentration was reduced [10, 11], causing a change in the proportions of the two mechanisms which was apparent as a decrease in the *x*-value. With the zincate system, the mechanism does not show any strong trend with hydroxide concentration. This suggests there is either just one mechanism of copper rearrangement, or that both copper dissolution and diffusion are reduced by the same amount as the hydroxide concentration varies, thus keeping the proportion constant. However, as previously mentioned [10, 11], copper diffusion would not be affected by hydroxide concentration whereas copper dissolution would, so it is unlikely that both mechanisms would be reduced at the same rate by varying the hydroxide concentration. A single mechanism is more likely. Figure 8 shows that in the presence of zincate the *x*-value is also not affected by temperature.

Increasing zincate concentration decreases the *x*-value linearly (Figure 9). This compares to a saturation-type effect with increasing chromate [11] that was due to the relative amounts of the two rearrangement mechanisms changing. At the highest zincate concentration in Figure 9, the value for *x* is about 0.2, well below the lowest possible value for any of the four types of rearrangement mechanism. Such a low *x*-value means that a portion of the copper structure must not be rearranging at all, being 'locked' in position. At low zincate concentrations in Figure 9, the value for *x* is higher than one third, which is the maximum possible value for a diffusion mechanism. Thus the copper dissolution mechanism must be operating in this system.

Given this information, and the evidence for a single mechanism from the hydroxide independence of *x*, the

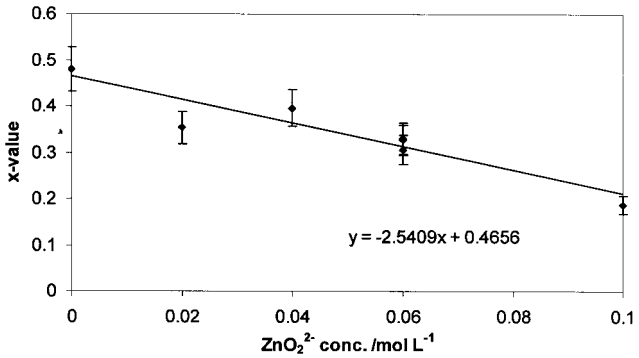

Fig. 9. The *x*-value varies linearly with zincate concentration.

structure in the zincate system is most likely controlled solely by copper dissolution/redeposition. The linear decrease in *x* with increasing zincate concentration must be due to progressively more of the copper structure being locked into position, hindered from rearrangement.

3.4. *The zincate mechanism*

Given that the zincate ions cannot be reduced to zinc metal at the mixed corrosion potential [12, 13], they must be precipitating as zinc oxide. This process is controlled by pH, and must be caused by the local consumption of hydroxide by aluminium dissolution at the reaction front. As might be expected, since there is a large excess of hydroxide, the zinc oxide precipitate will be prone to redissolution once the reaction front has passed. So, there are two main differences for zincate compared to chromate: namely, pH control instead of electrochemical reduction, and the ability to redissolve (the chromic oxide is only very slightly soluble [11, 12]).

The precipitation of zinc oxide is known to cause an increase in surface area by creating a finer copper structure [9]. Similar to the chromate system, the precipitated oxide must hinder the copper rearrangement. However, in this case the zincate must stop the copper diffusion altogether and hinder the copper dissolution/redeposition with increasing zincate

concentration. Elimination of copper diffusion may arise from the fact that the zinc oxide precipitate is concentrated at the leach front, becoming intimately mixed with the copper in its finest state and inhibiting its diffusion. Heavy precipitation of the oxide at the leach front would explain why the leaching rate was reduced to a greater extent in the presence of zincate compared to both the undoped and chromate-doped systems.

The redissolution of the zinc oxide is important. By taking away the stabilising oxide, the copper is free to rearrange once more. This is seen in the surface area results of Ma et al. [9] which show that the zincate system loses surface area with time whereas the chromate system produces a constant surface area.

It is interesting to test for a dependence between the rate of rearrangement and rate of dissolution. Such a relation can arise from a slower leaching rate causing less copper defects, which in turn slows rearrangement [16, 17]. By following the same procedure from the chromate work [11], the intercept of E against $\ln(t)$ is

$$int = -\frac{RT}{\alpha_{H_2,Cu} n_a F} \ln\left(\frac{3A_{disc} k_r (1-x)}{2k^0_{H_2,Cu} r_{L,0} K}\right) + E^{0'}_{H_2} \qquad (2)$$

The defect mechanism requires $k_r \propto k_d$, and so *int* must be proportional to $\ln(k_d)$ for this mechanism to be operative. A plot of *int* against $\ln(k_d)$ is shown in Figure 10 for different zincate concentrations. Similar to the chromate system [11], there is no obvious relationship, so the defect mechanism is either not present or not significant in this system.

Another possible co-mechanism is mentioned by Kalina et al. [18, 19], where a precipitated oxide might act as a nucleation source for the copper atoms. Increased nucleation sources create a finer structure. For this mechanism to be operating, the zinc oxide would exist *inside* the copper ligaments making up the skeletal copper. A separate publication [20] reports a method of detecting the location of additive species in this porous catalyst structure and shows that the zinc does reside inside the copper ligaments. This indicates that the zinc oxide acts as a nucleation source and is one of the reasons the structure is finer in the presence of zincate ions. The findings compare to the chromate system where the electron microscope results [20] showed that chromium resided primarily on the outside surface of the ligaments. The presence of zinc oxide inside the ligaments confirms the intimate mixing of copper and zinc oxide at the leach front, inhibiting structural rearrangement by copper diffusion. It also explains why not all of the zinc oxide redissolves after the leach front has passed [7, 8], rather a steady concentration profile exists throughout the leached residue.

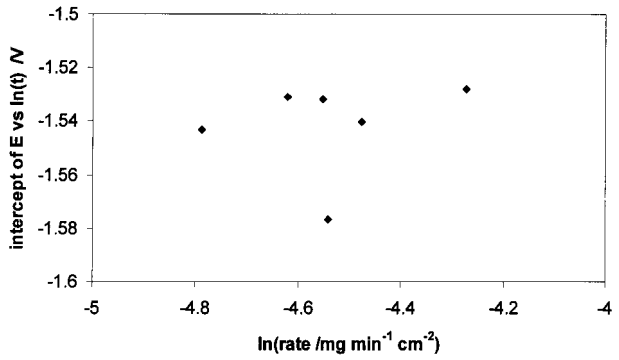

Fig. 10. There is no obvious relation between the intercept of E vs $\ln(t)$ and ln(dissolution rate).

The mixed corrosion potential of the zincate system did not rise steadily on a logarithmic curve with time, in contrast to experiments performed on other systems [10, 11]. Rather it oscillated, with a dip once or twice during the standard four-hour leaching period (Figure 11). This dip (mixed corrosion potential going more negative temporarily) corresponds to an 'apparent drop' in surface area and was reproducible. Since the aluminium dissolution rate remained constant and did not show a similar dip, the copper is still exposed at a constant rate. This suggests that the cause must be due to the zinc oxide precipitate, possibly passivating the surface from hydrogen evolution. The dip is rectified as the leach front moves on, causing the zinc oxide to redissolve. The fact that the dip(s) are only seen at the beginning of the leach time strengthens this argument, since they could only appear while the system was still stabilising. The dip did not affect the overall linearity of the E against $\ln(t)$ plots (Figure 6). It simply increased the scatter in the results slightly. Therefore the validity of Equation 1 still holds.

4. Conclusions

Zincate ions in the leaching solution decrease the aluminium dissolution rate to a greater extent than the chromate-doped system. There was no obvious dependence of leaching rate with sodium hydroxide concentration. However, a saturation-type effect was seen with increasing zincate concentration. The activation energy for leaching was found to be 84 ± 6 kJ mol^{-1}.

The mechanism of structural formation/rearrangement in the presence of zincate was found to be dissolution/reprecipitation of copper, with a complete

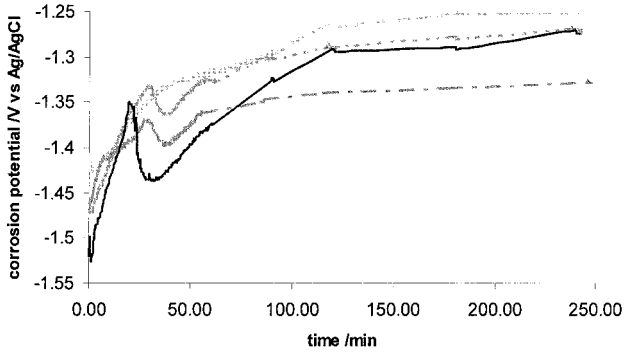

Fig. 11. Graph of mixed corrosion potential versus time for various concentrations of sodium hydroxide (0.06 M Na_2ZnO_2, 274 K). Key: (– – –) 2 M NaOH, (—-) 4 M NaOH, (------) 6 M NaOH and (——) 8 M NaOH.

absence of copper diffusion. The zincate ions precipitate onto the copper structure as zinc oxide, caused by a local fall in pH at the leach front. The precipitated oxide is intimately mixed with the copper atoms at the leach front, preventing copper diffusion.

By reducing copper rearrangement, the zincate caused a much finer leached structure. This structure had an increased surface area, and hence catalytic activity. However, since the precipitated zinc oxide redissolves when the leach front passes, the copper becomes free to rearrange again, as demonstrated by a decreasing surface area with time. Being inside the copper ligaments as well, not all of the zincate redissolves.

Acknowledgements

Financial support from the Australian Research Council is gratefully acknowledged. AJS is grateful to the Australian Government for receipt of an Australian Postgraduate Award. The authors also thank A/Prof. Paul Munroe and Ms Viera Piegerova, from the Electron Microscope Unit at UNSW, for their invaluable assistance in obtaining the micrographs. Thanks also to Brian Cooper for the casting work and Gautam Chattopadhyay for assistance with the ICP analysis.

References

1. M. Raney, *Ind. Eng. Chem.* **32**(9) (1940) 1199.
2. B.V. Aller, *J. Appl. Chem.* **8** (1958) 492.
3. J.A. Stanfield and P.E. Robbins, 'Raney Copper Catalysts' *in* Proc. 2nd Int. Cong. Catal., Paris (1960), pp. 2579–99.
4. M.S. Wainwright, 'Raney Copper – A Potential Methanol Synthesis Catalyst' *in* 'Alcohol Fuels', Sydney, 9–11 Aug. (1978), p. 8–1.
5. W.L. Marsden, M.S. Wainwright and J.B. Friedrich, *Ind. Eng. Chem. Prod. Res. Dev.* **19**(4) (1980) 551.
6. J.B. Friedrich, D.J. Young and M.S. Wainwright, *J. Catal.* **80** (1983) 1.
7. H.E. Curry-Hyde, M.S. Wainwright and D.J. Young, *Appl. Catal.* **77** (1991) 75.
8. H.E. Curry-Hyde, M.S. Wainwright and D.J. Young, *Appl. Catal.* **77** (1991) 89.
9. L. Ma, D.L. Trimm and M.S. Wainwright, Promoted skeletal copper catalysts for methanol synthesis *in* 'Advances of Alcohol Fuels in the World', Beijing, China, 21–24 Sept. (1998), pp. 1–7.
10. A.J. Smith, T. Tran and M.S. Wainwright, *J. Appl. Electrochem.* **29**(9) (1999) 1085.
11. A.J. Smith, L. Ma, T. Tran and M.S. Wainwright, *J. Appl. Electrochem.*, in press (2000).
12. M. Pourbaix, 'Atlas of Electrochemical Equilibria in Aqueous Solutions', National Association of Corrosion Engineers, Houston, TX, USA (1974) Sections 10.1, 14.1 and 15.1.
13. S.G. Robertson, I.M. Ritchie and D.M. Druskovich, *J. Appl. Electrochem.* **25** (1995) 659.
14. A.D. Tomsett, H.E. Curry-Hyde, M.S. Wainwright, D.J. Young and A.J. Bridgewater, *Appl. Catal.* **33** (1987) 119.
15. A.D. Tomsett, D.J. Young and M.S. Wainwright, *Appl. Catal.* **35** (1987) 321.
16. I.D. Zartsyn, A.V. Vvedenskii and I.K. Marshakov, *Russ. J. Electrochem.* **30**(4) (1994) 492.
17. L.M. Kefeli, *Kinet. Katal.* **12**(6) (1971) 1514.
18. M.M. Kalina, A.B. Fasman and V.N. Ermolaev, *Kinet. Katal.* **21**(3) (1980) 813.
19. M.M. Kalina, A.B. Fasman and V.N. Ermolaev, *Deposited Doc., VINITI* **1022–80** (1980) 15 pp.
20. A.J. Smith, P. Munroe, T. Tran and M.S. Wainwright, *J. Mater. Sci.*, submitted (2000).